NEUMANN BOUNDED PARTITIONS OF EIGENFUNCTIONS

A Senior Scholars Thesis

by

ROSS BEMENT MCDONALD

Submitted to the Office of Undergraduate Research
Texas A&M University
in partial fulfillment of the requirements for the designation as

UNDERGRADUATE RESEARCH SCHOLAR

April 2008

Majors: Physics

Mathematics

NEUMANN BOUNDED PARTITIONS OF EIGENFUNCTIONS

A Senior Scholars Thesis

by

ROSS BEMENT MCDONALD

Submitted to the Office of Undergraduate Research
Texas A&M University
in partial fulfillment of the requirements for the designation as

UNDERGRADUATE RESEARCH SCHOLAR

Approved by:

Research Advisor: Stephen A. Fulling
Associate Dean for Undergraduate Research: Robert C. Webb

April 2008

Majors: Physics

Mathematics

ABSTRACT

Neumann Bounded Partitions of Eigenfunctions (April 2008)

Ross Bement McDonald
Department of Physics
Department of Mathematics
Texas A&M University

Research Advisor: Dr. Stephen Fulling
Department of Mathematics

A new partitioning scheme, analogous to nodal domains, for the eigenfunctions of differential operators is constructed. The new scheme produces subdomains with Neumann boundaries instead of Dirichlet boundaries and will not experience an intersection avoidance phenomenon. General properties of this scheme are studied in 1 and 2 dimensions for various operators. First, a construction of the new scheme is given by providing definitions. Then numerical data is presented, and the properties of the new domains are studied. Finally, general properties are derived from the data and definitions.

To my mother and father

ACKNOWLEDGMENTS

I would like to thank my advisor, Dr. Stephen Fulling, for his continued guidance and input. I would also like to thank Dr. Thomas Hoffman-Ostenhof of the University of Vienna for providing direction early on, and all of my professors in the department of mathematics for providing me with the knowledge necessary to do this research. Finally, thanks to the National Science Foundation; this research was funded in part by NSF Grant PHY-0554849.

TABLE OF CONTENTS

Page

Page

LIST OF FIGURES

FIGURE Page

CHAPTER I

INTRODUCTION

Motivation

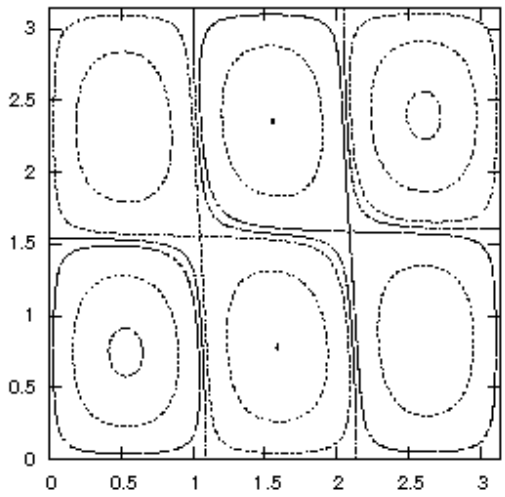

Figure 1. Contour plot of an example function.

A node of a function is a set of points in its domain at which the value of the function is 0. When these sets form continuous paths, they partition the domain of the function into subdomains called nodal domains. Figure 1 shows a contour plot describing the function $f(x, y) = \sin(3x)\sin(2y) + 0.2\sin(2x)\sin(3y)$. In figure 2, you can see how its nodes divide it up into its nodal domains.

This thesis follows the style of *Journal of Physics A*.

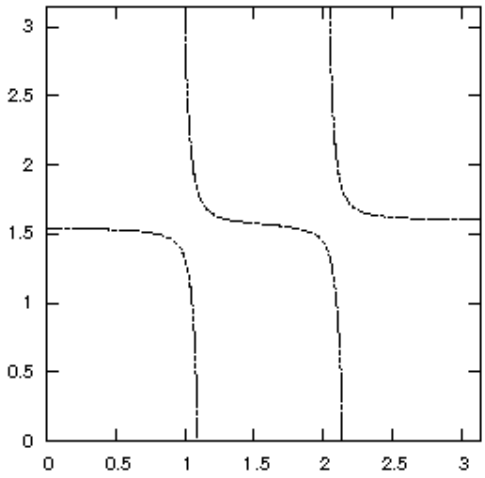

Figure 2. Nodal domains of an example function displaying intersection avoidance.

For years, the nodal domains of functions have been studied to reveal general properties of various classes of functions. Courant and Hilbert[1] showed that the first eigenfunction of a set is characterized by an absence of nodes and that all other eigenfunctions orthogonal to it would have nodes. Monastra, Smilansky, and Gnutzmann [2] showed that whether a system was chaotic or integrable could be related to the morphology of the eigenfunction's nodal sets.

However one interesting point is found in a paper by Chen, Fulling, and Zhou[3]: In 1 dimension, the nodal points of eigenfunctions of Sturm-Liouville operators form a kind of energy barrier and furthermore, the total energy of the system is divided

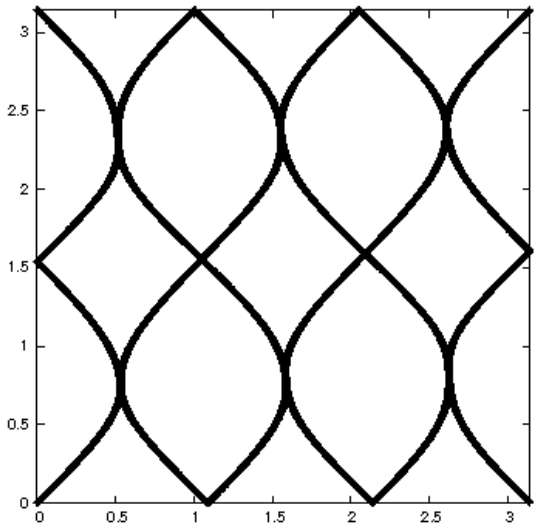

Figure 3. Proposed Neumann nodal domains of an example function.

equally among the nodal domains for sufficiently high frequencies. However these rather interesting properties are only very rarely extended to higher dimensions; this is mainly due to the fact that under slight perturbations, highly ordered nodal sets for which the equipartition is true blend together via an intersection avoidance phenomenon discussed by Monastra, Smilansky, and Gnutzmann[2]. Such an avoidance is demonstrated by figure 2 which is a plot of the nodal domains of the function in figure 1. In this avoidance, the saddle points at which the nodal intersections occur are still present, they just occur at nonzero values of the function. In the case of figure 1, they occur around the value ± 0.0864. In observing this, Chen, Fulling, and

Zhou[3] suggest that a different partition can be formed by connecting these saddle points in a more stable fashion and that such a partition may have this asymptotic equipartitioning of energy.

Which partitioning scheme should we examine? If we go back to the Sturm-Liouville eigenvalue problem examined by Chen, Fulling, and Zhou[3]:

$$[p(x)u'(x)]' + [\omega^2\rho(x) - V(x)]u(x) = 0, \quad a < x < b, \quad a, b \in \mathbb{R} \cup \{\pm\infty\}, \quad (1)$$

with their definitions of u's kinetic and potential energy on a subinterval $(\bar{a}, \bar{b}) \subseteq (a, b)$ respectively as:

$$KE(u; (\bar{a}, \bar{b})) = \omega^2 \int_{\bar{a}}^{\bar{b}} \rho(x)(u(x))^2 dx, \quad (2)$$

$$PE(u; (\bar{a}, \bar{b})) = \int_{\bar{a}}^{\bar{b}} p(x)(u'(x))^2 dx + \int_{\bar{a}}^{\bar{b}} V(x)(u(x))^2 dx, \quad (3)$$

Then multiplying through by $u(x)$ and integrating by parts gives

$$[u(x)p(x)u'(x)]_{\bar{a}}^{\bar{b}} + KE(u; (\bar{a}, \bar{b})) = PE(u; (\bar{a}, \bar{b})). \quad (4)$$

So, if $\bar{a}$ and $\bar{b}$ are nodes of u, that is $u(\bar{a}) = u(\bar{b}) = 0$, then the kinetic and potential energies are equal for this interval. However, also note that if $\bar{a}$ and $\bar{b}$ are so-called "Neumann" nodes of u, that is $u'(\bar{a}) = u'(\bar{b}) = 0$, then this is also true. Perhaps this is a partitioning scheme worth examining. Instead of looking at the nodal set of u, we can examine the nodal set of u'.

To extend this idea of Neumann nodes to higher dimensions, consider a partitioning scheme in which the boundaries of the partitions are Neumann boundaries, that is, the directional derivative of the function is 0 normal to the boundary. Since the directional derivative normal to the gradient is always zero, we can construct a new partitioning scheme of this Neumann nodal type in 2 dimensions by connecting all the saddle points of a function with paths that follow the gradient. A plot of these proposed Neumann nodes for the function in figure 1 is given in figure 3. In this paper, the properties of these Neumann partitions will be explored.

Preliminary definitions

In this section, several definitions are presented that will be used throughout this paper. For the following definitions, let $u : \Omega \to \mathbb{R}, \Omega \subseteq \mathbb{R}^n, n \in \mathbb{Z}^+$, with Ω open and connected in $\mathbb{R}^n$, be a function with continuous first and second order partial derivatives on Ω.

Definition 1 (Nodal Set) *The set $\mathcal{N}_u$ defined by*

$$\mathcal{N}_u = \{p \in \Omega | u(p) = 0\}$$

is called the nodal set of u.

Definition 2 (Nodal Domain) *Any set $A \subseteq \Omega \setminus \mathcal{N}_u$ such that A is connected and no other connected subset of $\Omega \setminus \mathcal{N}_u$ contains A is called a nodal domain of u.*

Definition 3 (Neumann Node) *If $n > 1$, a set $A \subseteq \Omega$ is a Neumann node of u if and only if A is a manifold of dimension $n-1$ embedded in Ω and for every point $p \in A$, $N_p \cdot \nabla u = 0$ where N_p is the unit normal vector of A at p. If $n = 1$, then a point $p \in \Omega$ is a Neumann node of u if and only if $u'(p) = 0$.*

Definition 4 (Neumann Nodal Set) *A Neumann nodal set of u is any union of one or more Neumann nodes of u.*

Definition 5 (Proper Neumann Node) *Let the set A be a Neumann node of u. A is a proper Neumann node if and only if there exists a point $p \in A$ such that p is a saddle point of u.*

Definition 6 (Proper Neumann Nodal Set) *The unique proper Neumann nodal set, $\mathcal{A}_u \subseteq \Omega$, of u is defined as the set that is the union of all proper Neumann nodes of u. However, for the case $n = 1$, it is defined as the set*

$$\{p | p \in \Omega \text{ and } u'(p) = 0\}$$

since u cannot have saddle points if it is a function of only one real variable.

The following 2 definitions apply only for the special case of $n = 2$:

Definition 7 (Gradient Neumann Node) *Let $\alpha : S \to \Omega$, where $S \subseteq \mathbb{R}$ and is connected and open. The image $\alpha[S]$ is a gradient Neumann node if and only if*

$\forall s \in S, \dot{\alpha}(s) \cdot \nabla u(s) = \pm|\dot{\alpha}(s)||\nabla u(s)|$ *and* $\exists p \in \alpha[S]$ *such that* p *is a saddle point of* u*; the Neumann node* $\alpha[S]$ *is said to be generated by the curve* α*.*

Definition 8 (Gradient Neumann Nodal Set) *The gradient Neumann nodal set of the function* u*, denoted by* $\mathcal{G}_u$*, is defined as the union of all gradient Neumann nodes of* u*.*

CHAPTER II

INVESTIGATION

One dimension

In one dimension, it is fairly easy to study the Neumann nodal domains of a given function. Consider a function $u : \Omega \to \mathbb{R}$, for some open subset Ω of $\mathbb{R}$, that is differentiable on Ω. The set of points $\{p \in \Omega | u'(p) = 0\}$ forms a complete and proper Neumann nodal set of u. So, to study this partitioning, we need only study the movement of the function's critical points.

Introduction to the two dimensional problem

Since the original curiosity was found in studying solutions to Sturm-Liouville equations, which can be seen as the steady-state portion of wave equations of one spacial dimension, it seems logical to study the solutions of elliptic partial differential equations in higher dimensions since they are seen as the steady-state portions of wave equations of more than one spatial dimension. So, for the remainder of this paper, we will only be considering the eigenfunctions of 2-dimensional linear elliptic partial differential operators of real-analytic coefficients that have isolated saddle-points. This restriction gives the functions under investigation several nice properties such as: They are smooth as long as the coefficients of the operator are smooth, they

are real-analytic and admit a local power series representation and every defined point if the operator has real-analytic coefficients at that point, they admit unique continuations if the operator has real-analytic coefficients at that point, and their saddle-points are isolated[4][5].

Now, in two dimensions, the situation becomes slightly more complicated. There potentially exist an infinite number of curves in a given function's domain that are Neumann nodes of that function. One of the reasons for looking at the Neumann nodes was to avoid the domain merging caused by intersection avoidance. So, to limit the number of nodes and keep the intersections, we restrict our investigation to Neumann nodes that contain a saddle-point of the function. This gives rise to definition 5 of a proper Neumann node.

One can easily form these proper Neumann nodes in two dimensions by following curves of steepest ascent through saddle-points since the derivative of a function normal to its gradient is always zero. In fact, tracing curves of steepest ascent numerically is computationally very easy for well behaved functions like these.

So, it's very easy to find the proper gradient Neumann nodes, but how can we be sure there is not some piece of the proper Neumann nodal set that is not covered by the gradient nodes?

Theorem 1 *For any function* $u : \Omega \to \mathbb{R}$, $\Omega \subseteq \mathbb{R}^2$ *open and connected,* $\mathcal{G}_u = \mathcal{A}_u$.

Since at any point p in the image of a curve α that generates a Neumann node, $\nabla u(p) \cdot N_\alpha(p) = 0$, where N_α is the unit normal of α, either $\nabla u(p) = 0$ or $N_\alpha(p)$ is perpendicular to $\nabla u(p)$. Since the image of α must contain a saddle-point, and that saddle-point must be isolated, the image of α cannot simply be a collection of critical points and in general must be perpendicular to $\nabla u(p)$ for all points p in the image of α. So for all p in the image of α, $\dot{\alpha}(p)$ must be parallel or anti-parallel to the gradient of u at p. Therefore any Neumann node $N \in \mathcal{A}_u$ is also a member of $\mathcal{G}_u$ and hence $\mathcal{A}_u \subseteq \mathcal{G}_u$. Also, any member of $\mathcal{G}_u$ is by definition a Neumann node that contains a saddle-point of u, so $\mathcal{G}_u \subseteq \mathcal{A}_u$, and hence $\mathcal{A}_u = \mathcal{G}_u$.

So the problem of finding a function's proper Neumann nodal set can be reduced to tracing curves of steepest ascent out from saddle-points, or more formally:

Given a function $u : \Omega \to \mathbb{R}$, $\Omega \subseteq \mathbb{R}^2$, that is an eigenfunction of some elliptical partial differential operator, we must find all solutions $\alpha : \mathbb{R} \to \Omega$ of the system of equations

$$\frac{d}{dt}\alpha(t) = \nabla u(\alpha(t)) \tag{5}$$

where there exists a $t_0 \in \mathbb{R}$ such that $\alpha(t_0)$ is a saddle-point of u.

Analytical results of the laplacian

A simple test case that allows for easy application of analytical techniques are the eigenfunctions of the two dimensional Laplacian in Cartesian coordinates. So we will be examining the set of eigenfunctions

$$u(x, y) = \sin(nx)\sin(my) \tag{6}$$

that solve the eigenvalue problem

$$\nabla^2 u = -\lambda u, \tag{7}$$

where $\lambda = n^2 + m^2$, on the whole real plane. Because of the repetitive nature of these functions, we can study the entire real plane by limiting our view to just the rectangle from $(0, 0)$ to $(\frac{2\pi}{n}, \frac{2\pi}{m})$.

First, let's take a look at the standard nodal domains of these functions. There are two representative cases I will look at now: $n = m = 1$ and $n = 2 > m = 1$. Also, for simplicity in comparing the graphs, and so that nodal crossings appear on the interior of the plot, each graph will be plotted on the square region of side length π with left bottom vertex at $(0, 0)$.

These functions are the nice type of function in which nodal crossing occurs. In figures 4 and 5, all of the nodal crossings occur on the boundary of the plots. As you can see, every domain is a reflection of every other domain. So, just about every

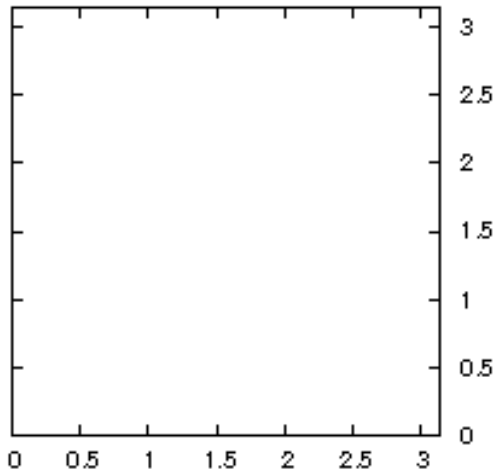

Figure 4. Nodes of $\sin(x)\sin(y)$.

quantity you can think of is equipartitioned by the nodes.

Now lets take a look at the proper Neumann nodes for these functions. They can be easily found by reducing the system in equation 5 to the single differential equation

$$\frac{dx}{dy} = \frac{\partial u/\partial x}{\partial u/\partial y} \tag{8}$$

and picking the saddle-points at $(0,0)$, $(\frac{\pi}{2},0)$, and $(\pi,0)$ to be the points of origin. Solving equation 8 gives the paths

$$x - x_0 = \frac{n}{m}\arccos(\cos(y-y_0)^{m^2/n^2}) \tag{9}$$

which are plotted in figures 6 and 7. For $n = m = 1$, the domains are nice and uniform

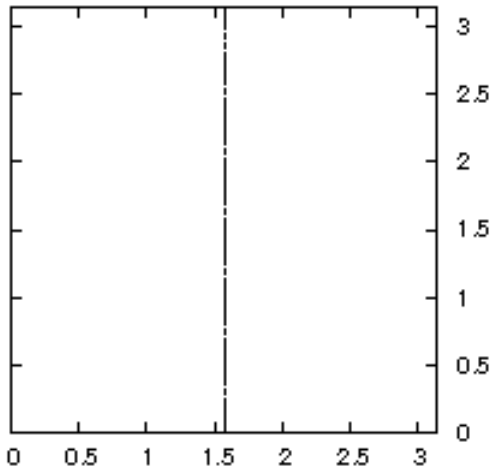

Figure 5. Nodes of $\sin(2x)\sin(y)$.

like their corresponding nodal domains, but for $n = 2 > m = 1$, two different shapes of domains form that do not equipartition the energy of the system. However, the formed domains appear stable and have the desired intersections.

Numerical methods

In more general cases, analytical solutions to equations 5 and 8 will not be possible. However, we can construct approximations using simple first order method in two

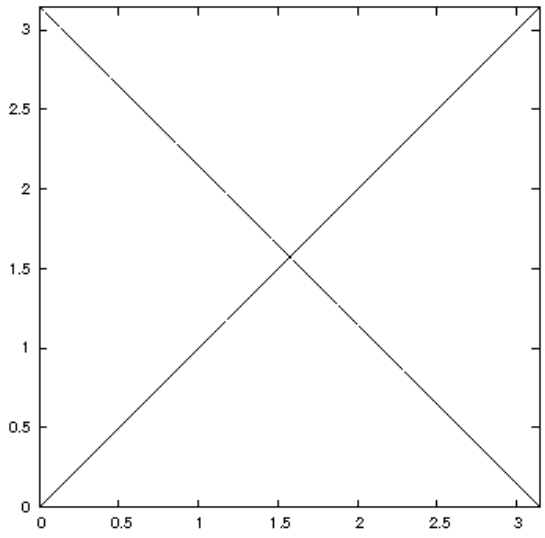

Figure 6. Neumann nodes of $\sin(x)\sin(y)$.

dimensions. The method used was the following iterative method:

$$x_{n+1} = x_n + \delta u_x(x_n) \tag{10}$$

$$y_{n+1} = y_n + \delta u_y(y_n). \tag{11}$$

This method will eventually converge on an extremum, but will not be able to procede through it.

However, tracing the gradient numerically like this will not work if we begin our iteration at the saddle-point since the gradient is zero there, and if we begin our iteration slightly off of the saddle-point, we will obtain only one of the four correct solutions. It turns out that in order to obtain all solutions needed, we will need

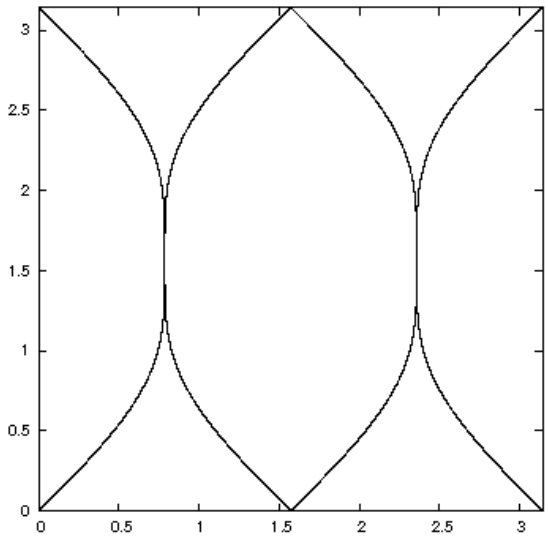

Figure 7. Neumann nodes of $\sin(2x)\sin(y)$.

to plot eight total iterations from four different points. For each originating point, one iteration must be run along the gradient and another against it. Each set of iterations from a point will locally form half a hyperbola centered on the saddle-point and will converge to the Neumann node as the distance of the points of origin from the saddle-point decreases. To ensure that the hyperbolas do not overlap, each point of origin after the first must be obtained by rotating the previous one $\pi/2$ radians about the saddle-point.

Superposition of degenerate eigenfunctions

In the example in the previous section, the functions were so well-behaved that we didn't get a chance to see if the Neumann nodes really were more stable. One of the features that caused the equipartitioning to fail in the normal nodal domains was the occurrence of domain blending by intersection avoidance. We would like to reconstruct this phenomenon in a test function to study. The standard rectangular eigenfunctions are too well-behaved to use, but by superposing two degenerate eigenfunctions, eigenfunctions that share the same eigenvalue, we can recreate the intersection avoidance while still dealing with functions that are easy to work with. As an example, we will look at the eigenfunctions of the Laplacian that solve

$$\nabla^2 u = -(n^2 + m^2)u; \tag{12}$$

specifically, the ones of the form

$$u(x, y) = \sin(t)\sin(nx)\sin(my) + \cos(t)\sin(mx)\sin(ny) \tag{13}$$

for $t \in [0, \pi/2]$. This way we cover all useful mixings of the standard eigenfunctions that are normalized to an amplitude of one.

In figures 8 through 17 we see the evolution of the nodal and Neumann nodal lines for the eigenfunctions of $n = 2$ and $m = 3$ for the values 0, 0.3, 0.7, 0.9, and $\pi/2$ respectively in t. The graphs show an immediate sign of intersection avoidance in the

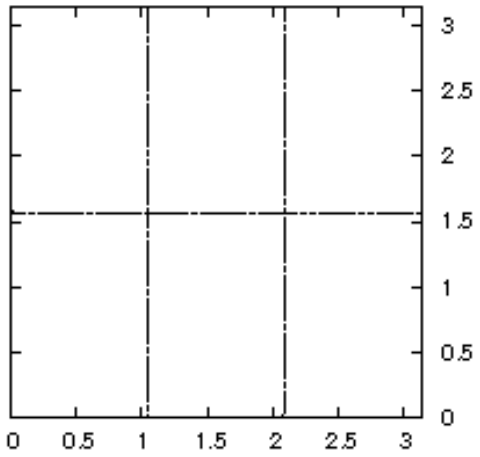

Figure 8. Nodes of $\sin(3x)\sin(2y)$.

nodal plots, but in the Neumann nodal plots, the intersections remain. For $t = \pi/2$, the nodal lines finally reconverge in an intersection, but for the whole evolution of t, the Neumann nodal intersections just seem to rotate around the center.

The Neumann nodes seem generally well-behaved, but there is an interesting occurrence between $t = 0.7$ and $t = 0.9$; the saddle-point intersections on the border of the graph rotate to a different side of the plot. This would seem to mean that those saddle-points coincided with the fixed saddle-points on the corners of the plot for some value of t. This finding is actually very important and will be fleshed out in more detail in chapter III.

Another interesting occurrence are the nature of the intersections themselves. In the

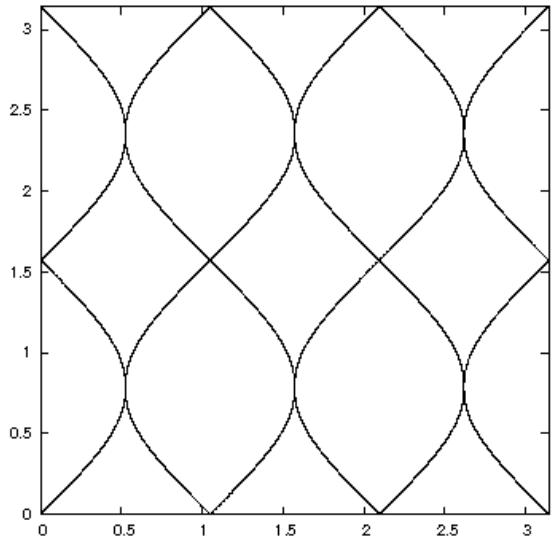

Figure 9. Neumann nodes of $\sin(3x)\sin(2y)$.

Neumann node plots in figures 9 through 17, all of the Neumann nodal intersections appear to happen at critical points of the function. Furthermore, all of the intersections at saddle-points seem to happen at right angles, and all of the ones at extrema are parallel and cusp-like. However, this cannot generally be the case; If we look back at figure 6, we can see that extrema intersections can also be at right angles. It turns out that this is the general result: Neumann nodal intersections that occur at non-degenerate critical points must be either at right angles or parallel. This will be shown to be true in chapter III.

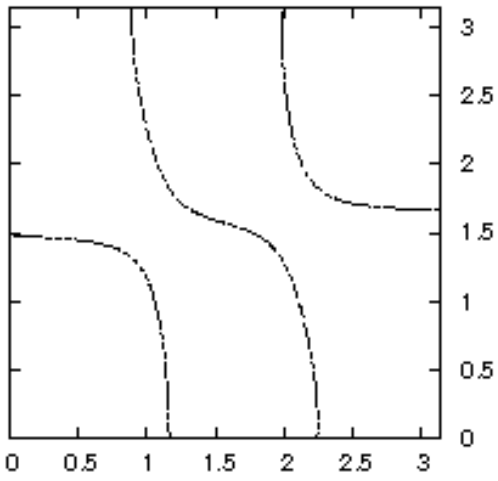

Figure 10. Nodes of $\sin(0.3)\sin(2x)\sin(3y) + \cos(0.3)\sin(3x)\sin(2y)$.

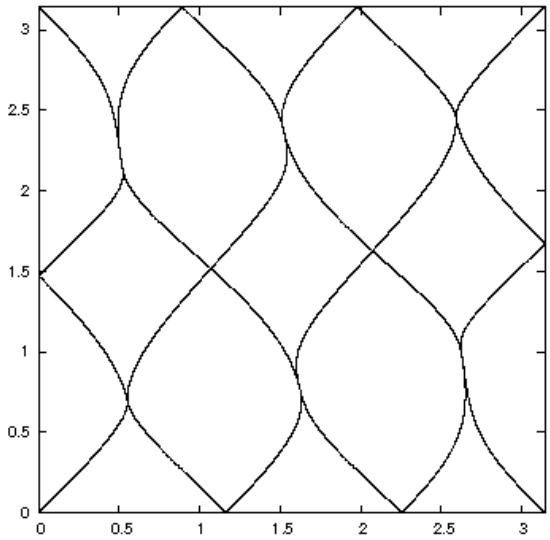

Figure 11. Neumann nodes of $\sin(0.3)\sin(2x)\sin(3y) + \cos(0.3)\sin(3x)\sin(2y)$.

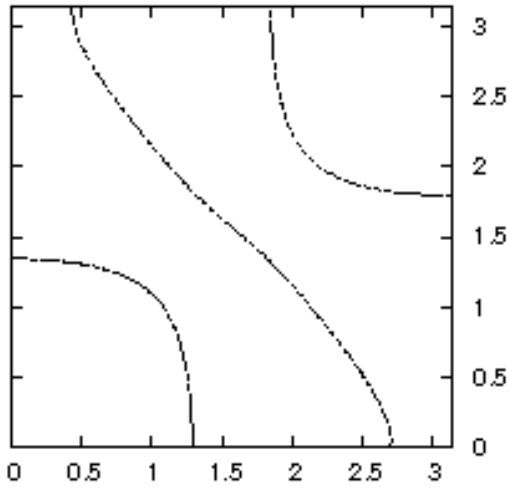

Figure 12. Nodes of $\sin(0.7)\sin(2x)\sin(3y) + \cos(0.7)\sin(3x)\sin(2y)$.

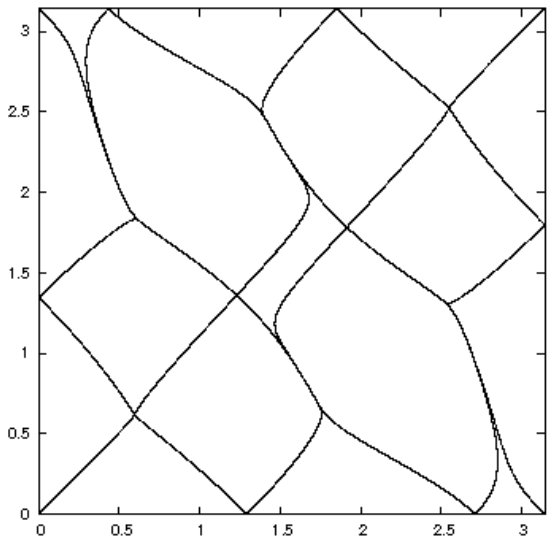

Figure 13. Neumann nodes of $\sin(0.7)\sin(2x)\sin(3y) + \cos(0.7)\sin(3x)\sin(2y)$.

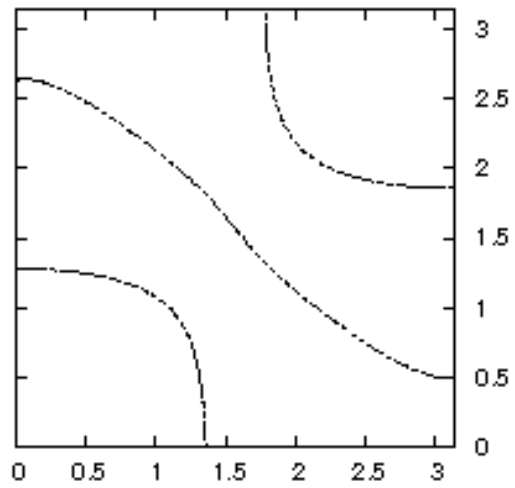

Figure 14. Nodes of $\sin(0.9)\sin(2x)\sin(3y) + \cos(0.9)\sin(3x)\sin(2y)$.

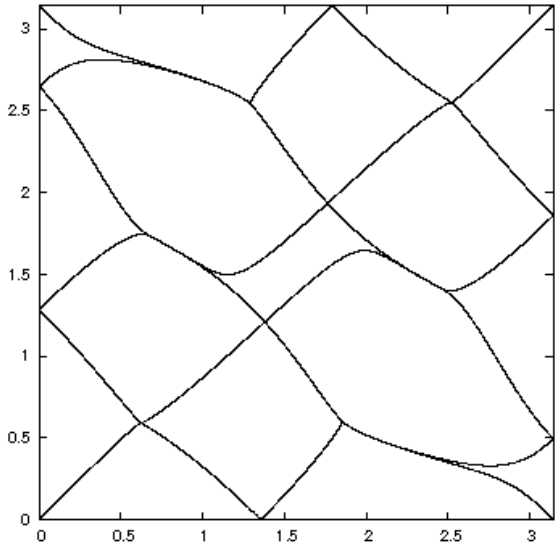

Figure 15. Neumann nodes of $\sin(0.9)\sin(2x)\sin(3y) + \cos(0.9)\sin(3x)\sin(2y)$.

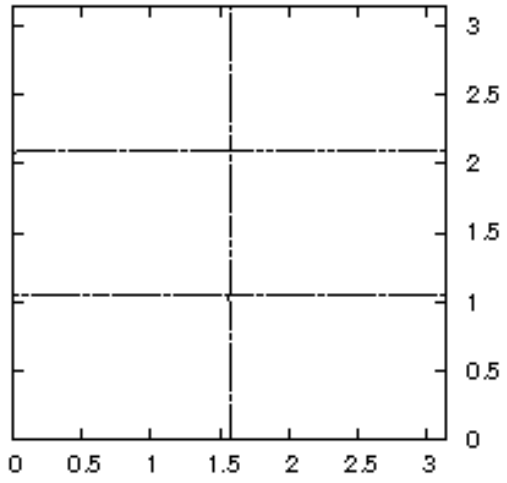

Figure 16. Nodes of $\sin(2x)\sin(3y)$.

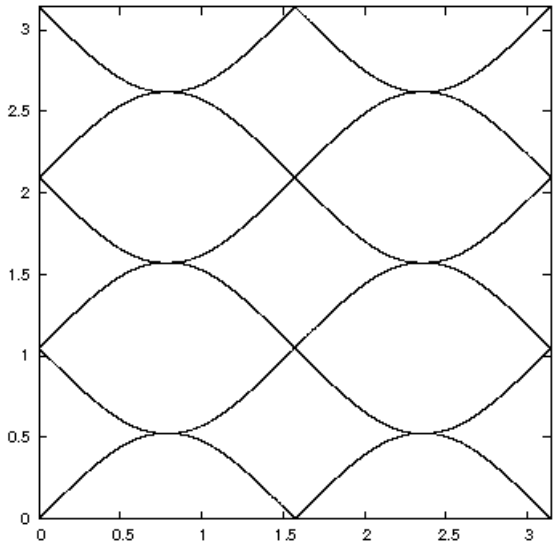

Figure 17. Neumann nodes of $\sin(2x)\sin(3y)$.

CHAPTER III

CONCLUSIONS

Energy equipartitioning

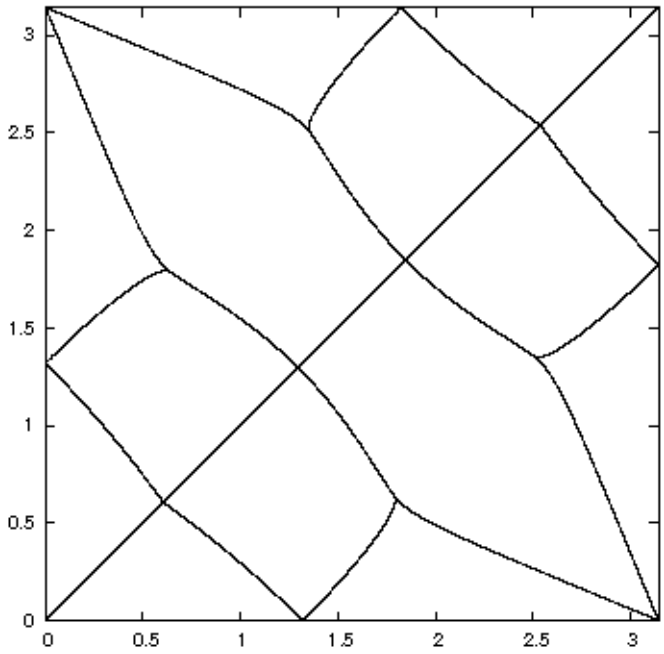

Figure 18. Neumann nodes of $\sin(\pi/4)\sin(2x)\sin(3y) + \cos(\pi/4)\sin(3x)\sin(2y)$.

In the evolution of t for the $n = 2$ and $m = 3$ superposition eigenfunctions, I showed that the saddle-points on the boundary of the plots rotated to a new side between figures 13 and 15. I also claimed that there must be a value of t for which those rotating saddle-points and the saddle-points fixed at the corners coincide. Figure 18

shows this particular occurrence.

When compared to the plots of these functions for other values of t, we can see that for this value of t, the central domain disappears. It actually shrinks down to a domain of zero area, so by picking a different values of t, we can make the size of this area arbitrarily small while the size of the other domains remain relatively unchanged and the function itself does not flatten out. So no value related to the square of the function on its domaincan be equipartitioned by the Neumann nodes, and therefore, Neumann nodes do not in general equipartition the energy.

Neumann nodal intersections

In the previous chapter, I mentioned that the Neumann nodal lines of a function can only intersect in certain ways. The intersections at non-degenerate critical points must be either at right angles or tangential. A non-degenerate critical point is a point at which all of the pure, non-mixed, second order partial derivatives are non-zero. The solutions to elliptic partial differential equations are nice enough that we can approximate them locally with a Taylor expansion. For the area around a non-degenerate critical point, we can look at the function's quadratic form at that point. If the critical point occurs at $(0, 0)$ in the (x', y') coordinates system, then the

quadratic form looks like:

$$u(x,y) \approx u_{x'x'}(0,0)(x')^2 + 2u_{x'y'}(0,0)x'y' + u_{y'y'}(0,0)(y')^2. \tag{14}$$

We can pick a new coordinate system that is just a rotation of the first which aligns itself along the quadratic form's principal axes[1]; this new coordinate system is (x,y), and in it, the quadratic form looks like:

$$u(x,y) \approx u_{xx}(0,0)x^2 + u_{yy}(0,0)y^2. \tag{15}$$

So around the saddle-point, the gradient Neumann nodal problem becomes

$$\frac{dy}{dt} \approx 2u_{yy}(0,0)y \tag{16}$$

$$\frac{dx}{dt} \approx 2u_{xx}(0,0)x \tag{17}$$

with $(x_0,y_0) = (x(0),y(0))$. We can solve this problem by integrating giving

$$\int_{y_0}^{y} \frac{dy}{y} \approx \int_0^t 2u_{yy}(0,0)dt \tag{18}$$

$$\int_{x_0}^{x} \frac{dx}{x} \approx \int_0^t 2u_{xx}(0,0)dt, \tag{19}$$

which yields the solutions

$$y \approx \pm y_0 e^{2u_{yy}(0,0)t} \tag{20}$$

$$x \approx \pm x_0 e^{2u_{xx}(0,0)t}. \tag{21}$$

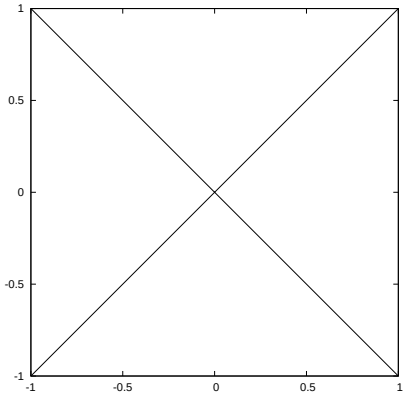

Figure 19. Example of Neumann nodal intersection for $u_{yy} = u_{xx}$.

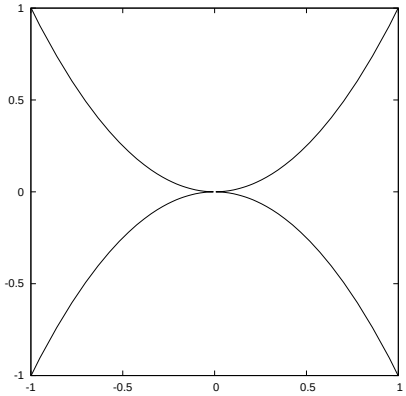

Figure 20. Example of Neumann nodal intersection for u_{yy} and u_{xx} of same sign but not equal.

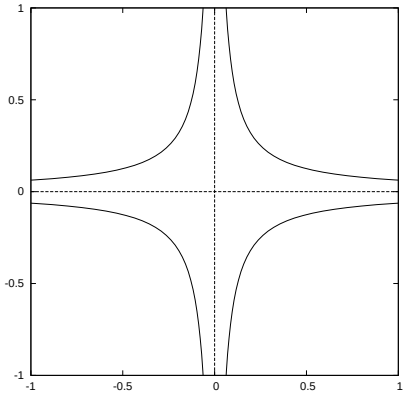

Figure 21. Example of Neumann nodal intersection for u_{yy} and u_{xx} of different sign.

In order to make these solutions proper Neumann node, they must originate at the saddle-point, but since we are using an integration to obtain them, we cannot use the saddle-point as the originating point; we must take the limit of the solutions as (x_0, y_0) approaches $(0, 0)$. These solutions can be broken into three classes: $u_{yy}(0,0) = u_{xx}(0,0)$, $u_{yy}(0,0)$ and $u_{xx}(0,0)$ are of the same sign but not equal, and $u_{yy}(0,0)$ and $u_{xx}(0,0)$ are of opposite sign. If they are equal, then the intersection occurs as two lines intersecting at a right angle as in figure 19. If they are not equal but of the same sign, then they intersect parallel to each other as in figure 20. If they are of opposite sign, then in general they do not intersect, but form a set of hyperbolas centered at the saddle-point, but when the limit of the origin point is taken, the hyperbolas converge to two lines intersecting at a right angle. Both of these situations are depicted in figure 21.

Since the sign of the second partial derivatives is all that is required to know the nature of the intersection, we can tie each type of intersection to a particular type of critical point. This confirms my statement in chapter II.

Theorem 2 *Two proper Neumann nodes intersecting at an extremum must intersect at either a right angle or parallel to each other.*

Theorem 3 *Two proper Neumann nodes intersection at a saddle-point must inter-*

sect at a right angle.

Conclusions

While Neumann nodal domains do appear much more stable than their regular counterparts in two dimensions, they did not fulfill the original purpose for their construction. In the previous chapter's section on the superposition of degenerate eigenfunctions, I showed that it was not reasonable to expect any kind of equipartitioning.

However, there were some interesting discoveries about the nature of the intersections between the Neumann nodes. Specifically, at non-degenerate critical points, they must intersect at either a right angle or parallel. I also presented useful information on how to construct complete proper Neumann nodal sets for functions of two dimensions for anyone else who might be interested in researching them.

REFERENCES

[1] Courant R and Hilbert D 1953 *Methods of Mathematical Physics* volume 1, New York: Interscience Publishers Inc.

[2] Monastra A G Smilansky U and Gnutzmann S 2003 *Journal of Physics A* **36** 1845

[3] Chen G Fulling S A and Zhou J 1997 *Journal of Mathematical Physics* **38** 5350

[4] Bers L 1964 *Partial Differential Equations* volume 3A of *Lectures in Applied Mathematics,* Rhode Island: American Mathematical Society

[5] Miranda C 1970 *Partial Differential Equations of Elliptic Type,* Berlin: Springer-Verlag

CONTACT INFORMATION

Name:	Ross Bement McDonald
Address:	Care of Stephen Fulling
	Department of Mathematics
	Texas A&M University
	College Station, TX 77843-3368
Email:	xenomorph64@tamu.edu
Education:	B.S. Physics, Texas A&M University, 2008
	B.S. Mathematics, Texas A&M University, 2008